Journal of Non-Crystalline Solids 355 (2009) 61–67

Contents lists available at ScienceDirect

Journal of Non-Crystalline Solids

journal homepage: www.elsevier.com/locate/jnoncrysol

Photosensitive defects in silica layers implanted with germanium ions

A.F. Zatsepin [a], H.-J. Fitting [b,*], V.S. Kortov [a], V.A. Pustovarov [a], B. Schmidt [c], E.A. Buntov [a]

[a] Department of Physics and Technology, Ural State Technical University, Mira Street 19, Ekaterinburg 620002, Russia
[b] Institute of Physics, University of Rostock, Universitätsplatz 3, D-18051 Rostock, Germany
[c] Research Center Dresden-Rossendorf, Institute of Ion Beam Physics and Materials Research, P.O. Box 510119, D-01314 Dresden, Germany

ARTICLE INFO

Article history:
Received 22 November 2007
Available online 12 November 2008

PACS:
61.46.Bc
61.72.Cc
68.37.Hk
68.37.Lp
68.55.Ln
78.60.Hk

Keywords:
Synchrotron radiation
Radiation effects
Defects
Optical properties
Absorption
Luminescence
Optical spectroscopy
Photoinduced effects
Time resolved measurements
Oxide glasses
Silica
Structure defects
Short-range order

ABSTRACT

Ge-implanted silica layers have been investigated by high-power pulsed synchrotron-photoluminescence (PL), photoluminescence excitation spectroscopy (PLE), and optically stimulated electron emission (OSEE) with respect to association of excitation and absorption bands to respective emission bands and lifetimes of excited defect states. In this way singlet–singlet (4.35 eV) and triplet–singlet (3.18 eV) radiative transitions from excited states of oxygen-deficient centers (ODC) in Ge-doped silica glass are characterized by their absorption and emission bands as well as their lifetimes. The main channel for non-radiative relaxation of photoexcitation is electron emission by the OSEE effect. The OSEE shows non-radiative transitions of surface E'_s and bulk E'-centers found with concentrations of $(2.7–3.4) \times 10^{12}$ cm^{-2} and $(2–4) \times 10^{16}$ cm^{-3}, respectively.

1. Introduction

Silicon dioxide has revealed as a very significant material for optics and microelectronics. The performance of optical and electronic devices, which are based on amorphous or crystalline SiO_2 considerably depends on the presence of excited states as well as intrinsic defects in the atomic SiO_2 network [1]. It is an established fact today that the so-called oxygen-deficient centers (ODC's) directly determine the sensitivity of such optical characteristics as the optical density and the refraction index to UV irradiation of 240–245 nm. This photosensitivity and the related photostructural transformations allow the production of Bragg-type superlattices in initially amorphous SiO_2. The study of these phenomena finds direct applications in optical recording of information, for manufacturing of photonic crystals, and other important techniques. However, photosensitivity mechanisms have not been clearly understood so far. This fact is explained to a large extent by the controversy of opinions as to the origin and the atomic and energy structures of ODC-type defects.

Optical absorption bands of SiO_2 near 5.0 and 5.2 eV and the associated luminescence bands at 3.1 and 4.4 eV, respectively, have been known for a long time [2,3]. However, the origins of these absorption bands and luminescent centers are not clear so far. The only evident fact is that all these bands correspond to some types of oxygen-deficient centers (ODC's). For example, the 5.02 and 5.15 absorption bands in pure SiO_2 (frequently referred to as $B_{2\alpha}$ and $B_{2\beta}$) are related to an oxygen vacancy ≡Si–Si≡ (V_O^0) and a twofold-coordinated silicon atom =Si: (Si_2^0), respectively [4,5]. A similar qualitative picture was observed in silica–germanate

* Corresponding author. Tel.: +49 381 498 6760; fax: +49 381 498 6802.
E-mail address: hans-joachim.fitting@uni-rostock.de (H.-J. Fitting).

0022-3093/$ - see front matter © 2008 Elsevier B.V. All rights reserved.
doi:10.1016/j.jnoncrysol.2008.08.025

glasses SiO_2:GeO_2 [6], but the 5.06- and 5.16-eV absorption maxima there were related to a vacancy ≡Ge–Ge≡ and a twofold-coordinated Ge_2^0 atom. Authors of later studies [7] held to the opinion that an oxygen vacancy should be absorbed at energies higher than 5 eV and a twofold-coordinated silicon atom =Si: possesses the absorption band at 5.2 eV. Thus, the origin of the maxima at 5.0 and 5.2 eV is not clearly understood. Hence, in the general case absorption bands of five types of oxygen-deficient centers can appear in the given spectra interval: oxygen vacancies ≡Si–Si≡ and ≡Ge–Ge≡; a mixed center ≡Si–Ge≡; and twofold-coordinated atoms of silicon =Si: and germanium =Ge:. Furthermore, some data point to a continuous distribution of spectral parameters of the bands in hand for one type of defect center [8]. The present study deals with specific features of excitation and relaxation of ODC's in SiO_2 films implanted with Ge ions.

2. Experimental technique

2.1. Samples under study

The samples were SiO_2 films (500 nm thick) on silicon substrate implanted by Ge^+ ions of energy 100 keV and fluence $\phi = 5 \times 10^{16}$ cm^{-2}. Afterwards the samples were thermally annealed at temperatures of 700, 900 and 1100 °C for 1 h in vacuum. Experimental details of the sample preparation had been given already in Ref. [9]. Finally, the samples were investigated by integral and time-resolved photoluminescence (PL) and optically stimulated electron emission (OSEE).

2.2. Luminescence measurements

Photoluminescence (PL) and photoluminescence excitation (PLE) spectra were measured on the SUPERLUMI station of HASYLAB/DESY in Hamburg/Germany under excitation by pulsed synchrotron radiation at temperatures of 9–10 K and 287 K. The luminescence spectra were obtained using an ARC Spectra Pro-308i monochromator and a R6358 P photomultiplier (Hamamatsu). By means of this monochromator the luminescence excitation spectra (PLE) were measured with a wavelength resolution of $\Delta\lambda = 3.2$ Å. Both the time-integrated luminescence and the time-resolved luminescence were detected, the latter one in time windows $\Delta t = 21$ and 72 ns with delays $\delta t_1 = 3.7$ ns and $\delta t_2 = 101$ ns, respectively, for the fast and slow components, see Fig. 1. The luminescence excitation spectra were normalized to an equal number of exciting photons using sodium salicylate for calibration. The obtained spectral dependences were approximated by a set of Gaussian functions, see e.g. Fig. 2.

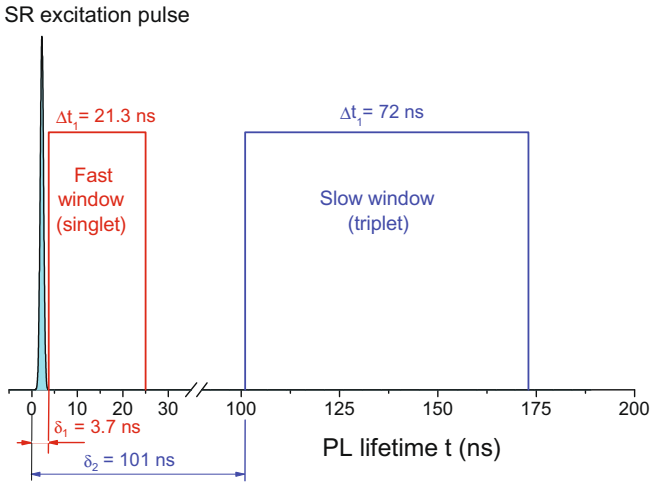

Fig. 1. Time-resolved photoluminescence measurement with a fast and a slow window mainly for the singlet and triplet registration, respectively. SR – synchrotron radiation.

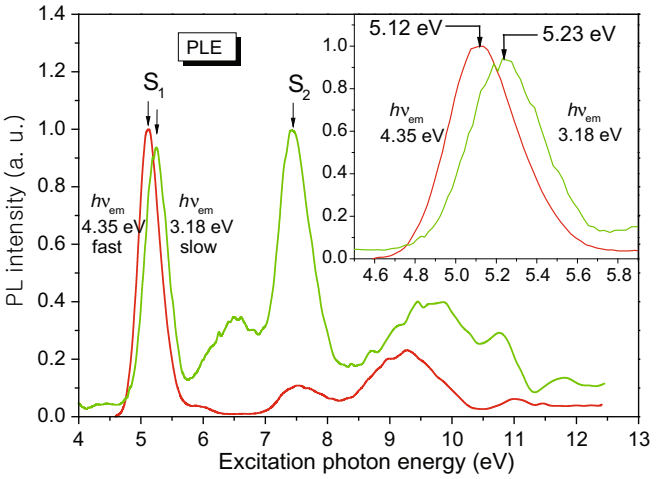

Fig. 2. Time-resolved PL excitation spectra of ODC's in SiO_2:Ge films with the singlet (4.35 eV) luminescence excitation, as the fast component; and the triplet (3.18 eV) luminescence excitation, as the slow component. The graph in the inset shows the first singlet state excitation peaks ($S_0 \rightarrow S_1$) on a larger scale.

2.3. Optically stimulated electron emission

OSEE spectra were measured under excitation of wavelengths $\lambda = 200$–260 nm. The UV source was a DDS-400 deuterium lamp. The required spectral interval was discriminated by a DMR-4 monochromator. A VEU-6 secondary electron multiplier was used to measure the electron flux intensity. The obtained non-selective spectral dependences were processed using original 'Photoelectron' and 'Spectrograph' software [10,11]. The method for processing of non-selective OSEE spectra is described in detail elsewhere [12,13]. Here in the following we describe only the main steps of the method. The contribution of electron emission from given defect centers present or induced in the silica matrix can be estimated if the spectral dependence is presented as a superposition of selective I_1 and non-selective I_2 components:

$$I(h\nu) = C'[I_1(h\nu) + I_2(h\nu)], \quad (1)$$

where C' is the parameter accounting for the influence of the radiation charging of the sample surface layer. $I_2(h\nu)$ is the non-selective component of the spectrum, which is due to photoionization of the band tail of surface states described well by the Uhrbach rule [14]. The selective component $I_1(h\nu)$ is approximated by a set of Gaussian functions. The approximation quality criterion was a sufficiently small standard deviation, whose numerical value depends on properties of samples under study and irradiation conditions.

After the spectra were resolved, concentrations N of the corresponding emission-active centers in the surface layer of the test material were determined from the intensity of each band using a modified Smakula formula in the emission form [4]:

$$N = 6.942 \times 10^{16} \frac{K \cdot S_{OSEE}}{f \cdot \eta \cdot h_{OSEE}}, \quad (2)$$

where S_{OSEE} is the integral intensity of an individual band, K is the instrumentation calibration constant, f is the optical transition oscillator strength, η is the photoemission quantum yield, and h_{OSEE} is the thickness of the emission-active layer of the sample.

3. Experimental results

The first experimental studies were extended to the excitation spectra of the so-called singlet (4.35 eV) and triplet (3.18 eV) luminescence. The spectral dependences shown in Fig. 2 exhibit excitation maxima of the first S_1 (5.1–5.2 eV) and second S_2 (7.5 eV) excited ODC singlet states. A considerable shift between the excitation peaks S_1 in the triplet and singlet states is seen. The spectral region of GeODC triplet PL excitation (6–7 eV) has a complex shape and constitutes the superposition of two elementary bands located at 6.3 and 6.7 eV. The former band is attributed to the surface E'_s-center and the latter to the triplet silicon cluster ≡SiSiSi≡ [15]. The spectral range 8.5–10 eV corresponds to the self-trapped and near-the-defect excitons in SiO_2.

Fig. 3 presents the excitation spectra of the singlet luminescence, the $S_1 \rightarrow S_0$ transition with emission energy of 4.35 eV. We have analyzed the spectra at energies of 4.7–6.5 eV. The main criterion for the resolution into Gaussian components was a minimum number of components. The available spectroscopic data for known bands [16] was considered and the condition for the corresponding resolutions of luminescence and OSEE spectra was fulfilled. It is seen from Fig. 3 that the resolved spectrum contains five bands of luminescence excitation. Their spectroscopic parameters as a function of annealing temperatures of the samples are given in Table 1. The most intense components at 5.00, 5.15 and 5.35 eV are noteworthy. FWHM of these bands (about 0.3 and 0.4 eV) are in good agreement with the literature data. To all appearance, weaker bands near 5.90 and 6.15 eV can be related to bulk and surface E'_s-centers. The intensity of the high-energy range of the spectrum was low and, therefore, the inset showing this range on a large scale was added to Fig. 2.

It is seen from Table 1 that positions of the maxima E and FWHM of the bands depend slightly on the annealing temperature. Small deviations of their positions are within the 2% accuracy of the resolution. At the same time, the intensity of the components changes significantly. The intensity of the bands in the low-temperature range of 4.7–5.7 eV exhibits an obvious extreme dependence on the temperature with the maximum near 900 °C, see Fig. 4. Less intense components have a monotonically increasing or decreasing dependence.

Excitation spectra of the triplet luminescence ($T_1 \rightarrow S_0$, emission energy of 3.18 eV) are presented in Fig. 5. In this case, the triplet luminescence is due to the intercombination conversions $S_1 \rightarrow T_1$ and $S_2 \rightarrow T_1$. The resolved spectrum also contains five components.

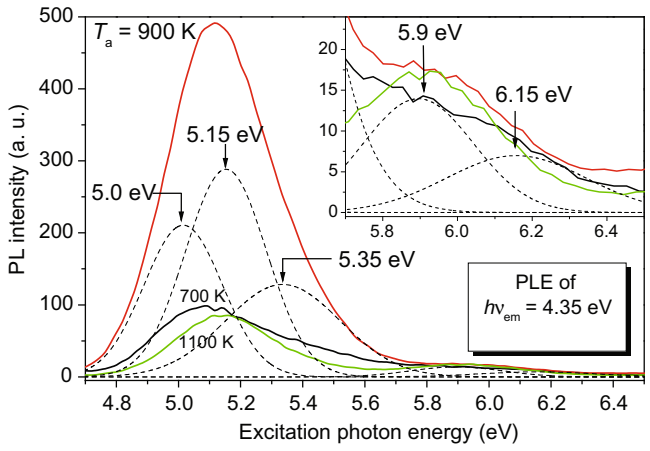

Fig. 3. Singlet ($h\nu$ = 4.35 eV) PL excitation spectra of SiO_2:Ge films after different annealing temperatures T_a = 700–1100 °C measured at T = 10.5 K. Dashed lines are Gaussian components of the spectra. The graph in the inset shows the higher spectra range on a larger scale.

Table 1
Parameters of the singlet PL excitation bands as given in Fig. 3. S – integrated band intensities in arb. units.

Centers	Parameters	Annealing temperature T_a (°C)		
		700	900	1100
5.00 eV (α-ODC)	E (eV)	5.00	5.01	5.01
	FWHM (eV)	0.30	0.30	0.30
	S (a.u.)	1748	6677	706
5.15 eV (β-ODC)	E (eV)	5.14	5.15	5.15
	FWHM (eV)	0.31	0.31	0.30
	S (a.u.)	1563	9419	1969
5.35 eV (h-ODC)	E (eV)	5.39	5.33	5.35
	FWHM (eV)	0.44	0.43	0.44
	S (a.u.)	1883	5940	1024
5.90 eV (?)	E (eV)	5.85	5.90	5.90
	FWHM (eV)	0.35	0.35	0.35
	S (a.u.)	404	517	579
6.15 eV (E'_s)	E (eV)	6.14	6.16	6.15
	FWHM (eV)	0.44	0.44	0.44
	S (a.u.)	349	326	226

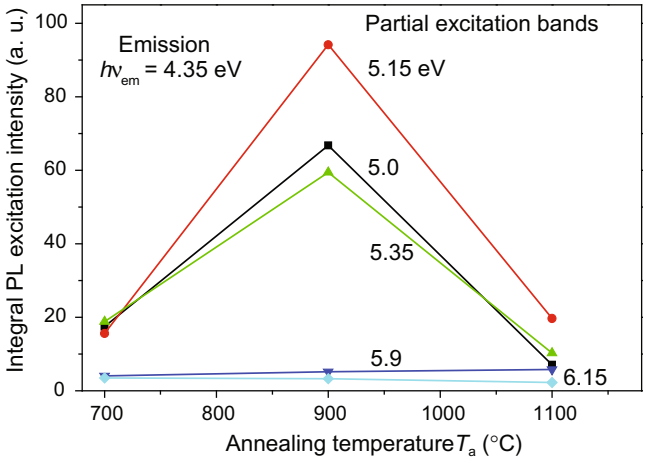

Fig. 4. Integral PLE band intensities in dependence on annealing temperature T_a, for the partial excitation bands; sample temperature T = 10.5 K.

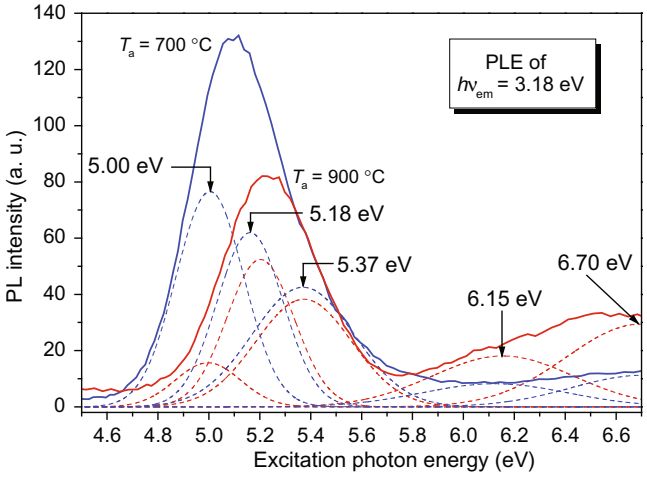

Fig. 5. Triplet (3.18 eV) PL excitation spectra of SiO_2:Ge samples measured at 286 and 10 K for samples annealed at 700 and 900 °C, respectively. The dashed lines are Gaussian components of the spectra.

Unlike in the singlet luminescence, the band at 5.9 eV is not observed. Moreover, a relatively wide maximum near 6.7 eV appears

additionally. It is seen from Fig. 5 that parameters of all the bands take different trends when the observation temperature and the annealing temperature change. The intensity of the 5.00-eV band changes sharply. The intensity of the maximum at 5.18 eV also follows the temperature. Moreover, this band shifts for 0.04 eV on the energy scale. At the same time, the intensity of the peak near 5.37 eV changes insignificantly. The intensity of the bands in the high-energy range of the spectrum has the opposite temperature dependence. This fact can be explained by the lower efficiency of the intercenter energy transfer or the development of competing processes.

Fig. 6 presents spectra of the stationary and fast luminescence of samples at 2.6–4.6 eV. The obviously non-elementary maximum near 3.1 eV corresponds to the triplet luminescence ($T_1 \rightarrow S_0$ transition) and the peak near 4.3 eV to the singlet luminescence ($S_1 \rightarrow S_0$). The fast and static components were chosen for the resolution of the singlet and triplet parts, respectively. Each of these parts of the spectrum was resolved into three components. The low-energy range contains bands at 2.73 and 3.15 eV, which are usually related to α-ODC(II) and β-ODC(II) (in our interpretation, SiODC and GeODC, respectively), and the intermediate peak at 2.92 eV. The components at 4.25, 4.32 and 4.49 eV are present in the singlet range.

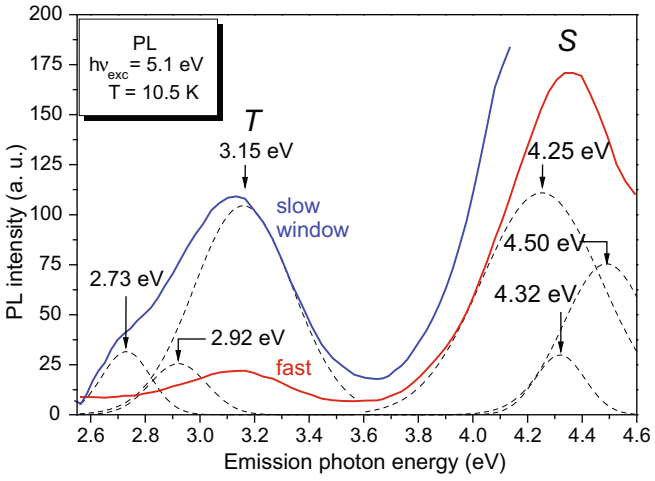

Fig. 6. Time-resolved photoluminescence spectra of ODC's in SiO_2–Ge samples annealed at T_a = 700 °C showing the slow (*T*: triplet) and the fast (*S*: singlet) components. The dashed lines are Gaussian components of the spectra; excitation $h\nu_{exc}$ = 5.1 eV; sample temperature *T* = 10.5 K.

Fig. 7 presents kinetic curves of the singlet luminescence at different annealing and observation temperatures. The decay kinetics at the annealing temperature of 700 °C is described well by three exponential functions, while two exponents suffice for approximation of the other curves. All the resolved kinetic curves contain exponents having the characteristic decay time of about 2.4 and 7.4 ns. An additional exponent with the decay time of 20 ns is observed at the annealing temperature of 700 °C. This fact probably points to the presence of the corresponding additional type of defect centers.

Fig. 8 shows selective OSEE spectra of the same samples, which were measured at room temperature. It is seen that the 6.04 and 6.27 eV bands, which may be related to surface $E'_s(2)$ and $E'_s(1)$ centers, see Ref. [17], dominate with respect to their intensity at any annealing temperature. Similarly to the luminescence measurements, the low-energy range contains bands at 5.00, 5.17 and 5.35 eV. These OSEE peaks are well conformed with corresponding singlet and triplet ODC PL excitation bands. In addition to the aforementioned components, the resolved OSEE spectra include the maximum at 5.70 eV, which may be tentatively related to bulk *E*′-centers. The location and the FWHM of the emission bands are constant within the resolution error. The dependence of their intensity on the annealing temperature is shown in Fig. 9. The intensity of the bands in the low-energy range has a minimum near 900 °C, i.e. its behavior is non-symptomatic with respect to the luminescence intensity. The intensity of the OSEE bands at 5.37, 6.04 and 6.27 eV has a clear trend to decrease with growing annealing temperature.

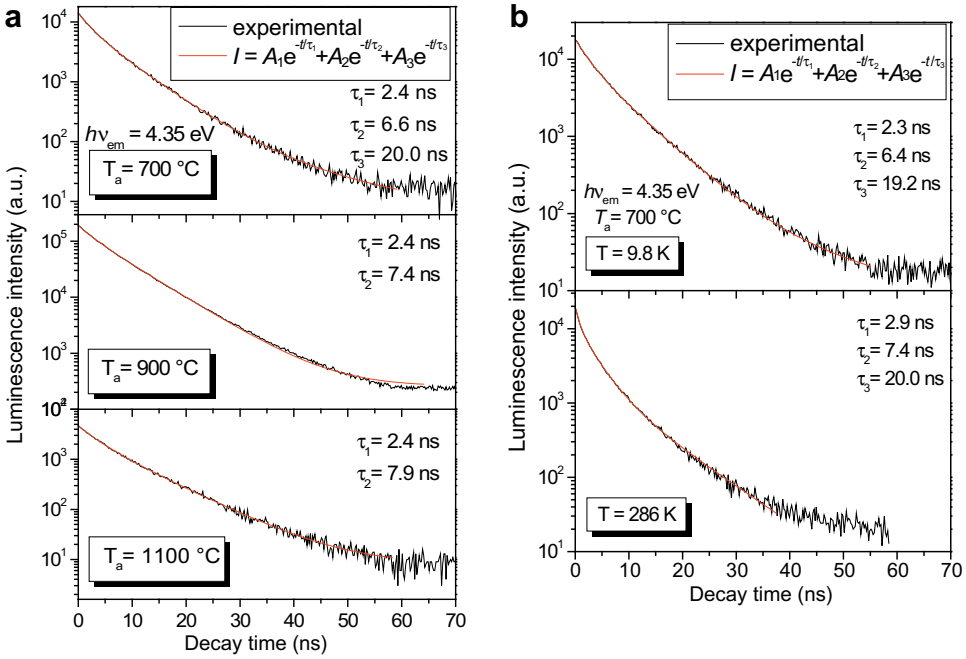

Fig. 7. Experimental and fitted decay kinetics of the singlet (4.35 eV) luminescence for an excitation energy of 5.1 eV in SiO_2:Ge samples. (a) Samples annealed at different temperatures T_a = 700–1100 °C, PL measurement temperature *T* = 10.5 K; (b) sample annealed at T_a = 700 °C, measurement temperatures *T* = 9.8 and 286 K.

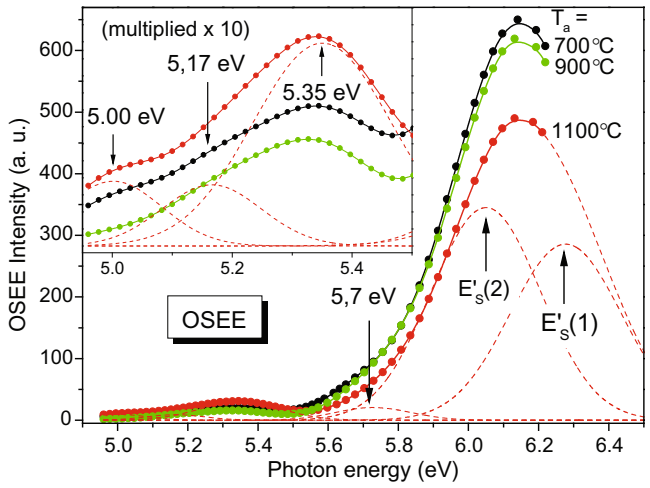

Fig. 8. OSEE spectra of SiO_2:Ge samples annealed at different temperatures T_a = 700–1100 °C. The dashed lines show Gaussian components of the spectra. The graph in the inset shows the lower spectra on a larger scale.

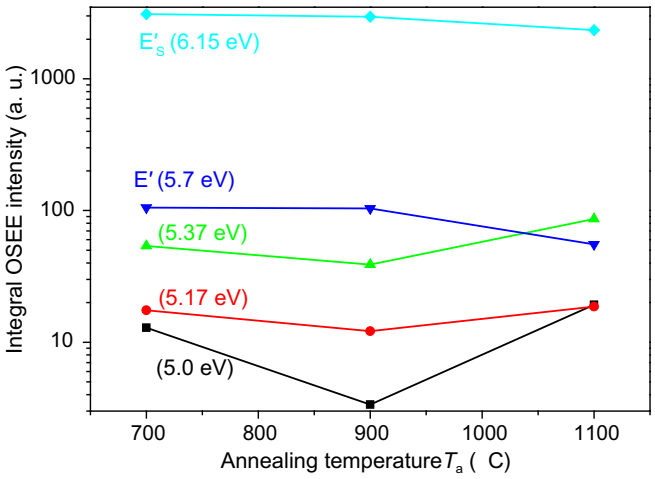

Fig. 9. Integral OSEE band intensities and their association to surface E'_s and bulk E'-centers in dependence on the annealing temperature T_a.

4. Discussion

Two intense maxima of luminescent defects near 5.1 and 7.4 eV are clearly seen in the luminescence excitation spectra of Fig. 2. If excitation is realized at these wavelengths, the luminescence intensity increases in the region, which is characteristic of the radiative relaxation of singlet (4.35 eV) and triplet (3.18 eV) excited states of ODC's [16]. Therefore, it may be stated that the two luminescence excitation maxima correspond to one type of oxygen-deficient centers (ODC). In our interpretation, these bands refer to the excitation of the first $S_0 \rightarrow S_1$ transition (5.1 eV) and secondly to the $S_0 \rightarrow S_2$ excitation (7.4 eV) of ODC's.

The observed high-energy shift of the peak S_1 in the excitation spectrum of the triplet luminescence with respect to the corresponding peak in the singlet excitation spectrum may be due to the dominance of non-uniform broadening of these maxima. This means that the general contour of the luminescence excitation band is a superposition of narrower contours of separate centers of one type, which differ, however, by their parameters because of their inhomogeneous environment in the amorphous SiO_2 matrix. If the concentration of defect centers is large, one may observe their continuous distribution with respect to some parameters. The maximum of the total band corresponds to centers with the most efficient luminescence. Considering what has been said above, the explanation for the high-energy shift of the triplet luminescence excitation peak means that centers with a larger excitation energy are characterized by a highly efficient intercombination conversion $S_1 \rightarrow T_1$, i.e. with a lower potential barrier of the $S_1 \rightarrow T_1$ transition.

At the same time, it is seen from Fig. 3 that the excitation band at 5.1 eV is not an elementary band. Three components at 5.00, 5.15 and 5.35 eV dominate in this spectra range. The shift of the total band can be explained by redistribution of the component intensities. 'High-energy' centers, probably, have a relatively low potential barrier for the intercombination ($S_1 \rightarrow T_1$) conversion. This statement applies more to defects responsible for the bands at 5.15 and 5.35 eV and is confirmed by a weak temperature dependence of the intensities of these bands during the triplet excitation, see Fig. 5.

Since there is no consensus of opinions about the relation of the luminescence excitation bands near 4.8–5.4 eV, the identification of these maxima seems to be a rather complicated problem. Most probably, this range includes oxygen-deficient centers of different types. Parameters of the 5.0-eV band (FWHM = 0.3 eV) approach most to those of silicon ODC's [15]. In our interpretation, SiODC represents an oxygen vacancy ≡Si–Si≡. The analogous band at 5.15 eV (FWHM = 0.3 eV) can be tentatively referred to germanium ODC's. In this case, however, germanium centers may imply both ≡Ge–Ge≡ vacancies and mixed defects ≡Si–Ge≡. Spectroscopic parameters of the wider maximum at 5.37 eV are similar to those of ODC peaks and the temperature dependence of its intensity is analogous to the same dependence of the 'low-energy' bands, see Fig. 4. According to data of Ref. [17] its position corresponds to excitation energies of a twofold-coordinated germanium atom =Ge:.

A detailed analysis of the luminescence in the SiO_2–Ge samples, thermally annealed at 700 °C, demonstrates that the spectrum of the stationary triplet luminescence ($T_1 \rightarrow S_0$ transition) also contains three components at 2.73, 3.15 and 2.92 eV. The first two bands at 2.73 and 3.15 eV usually are related to α-ODC(II) and β-ODC(II), in our interpretation, SiODC and GeODC, respectively, see also [18]. The last band (2.92 eV) can be presumably interpreted as the triplet luminescence of an intermediate 'hybrid' h-ODC, which is formed in the atomic structure of the implanted sample during thermal treatment at 700 °C. The assumption that the presence of the third hybrid center correlates with the fact that the kinetic decay curve of the singlet luminescence ($S_1 \rightarrow S_0$) in this sample (700 °C) is approximated best by the sum of three components with the characteristic decay time τ_1 = 2.4 ns, τ_2 = 7.4 ns and τ_3 = 20 ns in distinction from the samples annealed at 900 °C and 1100 °C, in which the last exponential component with τ_3 is absent. The intermediate band does not show up in high-temperature luminescence spectra either. The comparison of the decay times in the samples annealed at 900 °C and 1100 °C, in which α-ODC's and β-ODC's dominate, suggests that the new 'hybrid' ODC corresponds to the slowest component with the decay time τ_3 = 20 ns. These PL decay data are more precise than former ones given for SiO_2:Ge samples in [19].

The radiative transition energy of 'hybrid' centers is the average over the corresponding energies of $S_1 \rightarrow S_0$ optical transitions for germanium and silicon ODC's. However, the origin of the 'hybrid' ODC cannot be related to a twofold-coordinated silicon atom since it is difficult to imagine a defect, which would be intermediate between =Si: and =Ge:. Therefore, if an ODC is modeled as a single neutral oxygen vacancy, one may think that the 'hybrid' center is a neutral oxygen vacancy between neighboring atoms of silicon and germanium in the structure of implanted SiO_2.

As the annealing temperature grows, the intensity of the β-ODC luminescence first increases, reaches the maximum near 900 °C, and finally decreases. This variation behavior of the β-ODC luminescent activity suggests that the local concentration of β-ODC's rises upon high-temperature annealing of the samples, showing up as the concentration quenching of the luminescence. We think this effect stems from the segregation of Ge atoms in the structure of the implanted SiO_2 film, their subsequent clusterization and the formation of corresponding nanocrystals (quantum dots). The general tendency of the thermally induced transformation of the atomic structure in SiO_2 films after post-implantation annealing of the samples may be pictured finally as the redistribution (mutual transformation) of different types of ODC's:

$$\mathrm{SiSi} \rightarrow \mathrm{SiGe} \rightarrow \mathrm{GeGe} \rightarrow \text{segregation} \rightarrow \mathrm{Ge} - \text{clusters (quantum dots)}$$

having been investigated more detailed in [20,21].

Excitation spectra of the singlet and triplet luminescence of ODC's also contain high-energy bands (5.89 and 6.15 eV). The maximum at 5.89 eV (FWHM = 0.35 eV) is observed only during the singlet excitation, while the 6.15-eV band (FWHM = 0.44 eV) is present in all the PLE spectra. The energy of the observed 5.9 eV PLE band is quite close to the well-known absorption peak attributed to bulk E'-centers. However, such a band is absolutely absent in OSEE spectra of studied samples. At the same time there is an emission band near 5.7 eV corresponding to the ionization of bulk E'_γ-centers [22,17]. This experimental evidence does not allow us to contribute the 5.9 eV PLE band to the optically active defects of E' type. The 5.8–5.9 eV band was observed by Nishikawa et al. [23] and Weeks et al. [24] in non-stoichiometric silica. They have attributed this band to non-paramagnetic defects. Thus the observation of the noted 5.9 eV band in the excitation spectra of SiO_2–Ge samples denotes the possibility of excitation energy transfer between different types of non-paramagnetic centers. These defects may be localized at the non-stoichiometric intermediate layer between the wafer and the oxide.

As it shown by OSEE spectroscopy, the 6.15 eV PLE band is non-elementary and consists of two peaks attributed to $E'_s(2)$ and $E'_s(1)$ centers which differ in the presence of a hydrogen impurity in the defect local structure [25]. These defects do not produce self-luminescence. This fact additionally point to the possibility of the energy transfer between different types of defect centers, namely from E'-centers to ODC's. A relatively wide band at 6.7 eV also appears during excitation of the triplet luminescence. Earlier in the work [15] it was shown that ODC's of surface type have well pronounced excitation bands in this spectral region of porous nanoceramics. The data obtained in the present work firstly allow us to assume the existence of surface GeODC in the studied films. Secondly it points to the possibility of this center luminescence excitation through surface E'_s-centers and ≡SiSiSi≡ cluster absorption bands. Thus, in this case the effect of energy transfer between different types of defect centers is taking place, namely from non-luminescent E' to luminescent ODC's. This conclusion is confirmed by the results of OSEE measurements.

Surface E'_s-centers are the dominant type of defects in the OSEE spectra. The corresponding bands are located near 6.04 and 6.27 eV and their FWHM is about 0.37 eV. It is known that the absorption band of several types of bulk E'-centers appears at 5.7–5.8 eV. Therefore, the observed emission peak may probably be related to one of these centers.

Considering all the measurement results, we presumably may define five main types of defect centers present in the samples studied. These defects and parameters of their corresponding luminescence bands are given in Table 2. Table 3 contains the corresponding emission parameters. The concentration N_v was calculated from the modified Smakula formula Eq. (2). The surface concentration of the surface E'_s-centers is given too. It was calculated from the bulk concentration by the formula

$$N_s = \frac{\sqrt[3]{(N_v \cdot f \cdot \eta)^2}}{f \cdot \eta}, \tag{3}$$

where N_s and N_v are surface and bulk concentrations, respectively.

The observed compliance of luminescent bands (5.00, 5.17 and 5.35 eV) spectroscopic parameters with respect to corresponding OSEE bands can be considered as additional evidence of three different ODC-types existence. It should be noted that FWHM of OSEE maxima are frequently much smaller than those of optical absorption and luminescence [16,18]. This circumstance may be explained by the fact that the thickness of the OSEE emission-active layer is small (less than 100 nm), i.e. the OSEE process involves just a small fraction of defect centers, leading to a considerable decrease in inhomogeneous broadening of spectral lines. Non-symptomatic temperature dependences of PL and OSEE bands intensity are due to the fact that radiation and photoionization processes are the alternative ways of defect's photoexcited state. In the general case, the lifetime of excited singlet states S_1 of the aforementioned types of ODC's depends on the probability P_{rad} of the radiative $S_1 \rightarrow S_0$ transition, the probability P_{conv} of the intercombination conversion ($S_1 \rightarrow T_1$), and the photoionization probability P_I:

$$\tau = 1/(P_{rad} + P_{conv} + P_I). \tag{4}$$

Table 3
Defect centers and their spectral parameters as determined by the method of OSEE spectroscopy.

Center	E (eV)	FWHM (eV)	N (cm^{-3}) 700 °C/1100
α-ODC	5.0	0.16	$6.6 \times 10^{15}/9.9 \times 10^{15}$
β-ODC	5.17	0.16	$1.9 \times 10^{16}/2.0 \times 10^{16}$
h-ODC	5.35	0.22	$5.9 \times 10^{17}/9.5 \times 10^{17}$
E'_γ	5.73	0.21	$4.1 \times 10^{16}/2.1 \times 10^{16}$
$E'_s(2)$	6.04	0.36	$1.8 \times 10^{12}/1.4 \times 10^{12}$ (cm^{-2})
$E'_s(1)$	6.27	0.37	$1.6 \times 10^{12}/1.3 \times 0^{12}$ (cm^{-2})

Table 2
Defect centers and their spectral parameters as determined by photoluminescence excitation (PLE) and photoluminescence (PL) spectroscopy; τ – PL lifetime.

Centers	PLE				PL				
	E (eV)		FWHM (eV)		E (eV)		FWHM (eV)		τ (ns)
	$S_0 \rightarrow S_1$	$S_0 \rightarrow S_1 \rightarrow T_1$	$S_0 \rightarrow S_1$	$S_0 \rightarrow S_1 \rightarrow T_1$	$S_1 \rightarrow S_0$	$T_1 \rightarrow S_0$	$S_1 \rightarrow S_0$	$T_1 \rightarrow S_0$	$S_1 \rightarrow S_0$
α-ODC	5.00	5.00	0.3	0.3	2.73	4.49	0.21	0.37	2.5
β-ODC	5.15	5.17	0.3	0.3	3.15	4.25	0.43	0.52	7.4
h-ODC	5.35	5.37	0.4	0.3	2.92	4.32	0.25	0.21	20
(?)	5.89	–	0.35	0.44	–		–		–
E'_s	6.15	6.15	0.44	0.65	–		–		–

Since experiments were performed at sufficiently low temperatures (~10 K), one may consider the condition $P_{conv} \ll P_{rad}$ is fulfilled in this case.

5. Conclusions

1. The analysis of the time-resolved photoluminescence and OSEE spectra of Ge-ion implanted SiO_2 films points to the presence of two groups of photosensitive oxygen-deficient defects in the film structure: (1) luminescent defects like ODC's and (2) non-luminescent E′-centers.
2. Defects of the first group refer to diamagnetic centers and are characterized by the triplet and singlet luminescence. The spectra-kinetic measurements allow to distinguish between the following species of defects in this group: α-ODC's (excitation band at 5.00 eV), β-ODC's (5.15 eV), and the so-called 'hybrid' h-ODC's (excitation band at 5.35 eV), which are interpreted in terms of a neutral oxygen vacancy model of ≡Si–Ge≡. Specific features of the transformation of luminescence-emission characteristics of ODC's during thermal annealing of SiO_2 films suggest the possible segregation of germanium ODC's and the formation of defect clusters at temperatures above 900 °C.
3. The group of non-luminescent defects in the implanted films includes E'-centers of the bulk and surface types. It is shown that the main channel for the non-radiative relaxation of the photoexcitation of the non-luminescent defects is ionization, which shows up as the OSEE effect. The dominant active centers of the photoelectron emission are surface E'_s-centers with a surface concentration of 4×10^{12} cm^2.
4. The experimental results point to the presence of an additional channel for the relaxation of optically excited surface E'_s-centers and non-paramagnetic defects by the intercenter energy transfer to defects like ODC's. A specific feature of this relaxation process is that the triplet luminescence of ODC's is excited only by the energy transfer from surface E'-centers, whereas singlet luminescence can be excited by both types of defects. It is shown that a non-radiative transfer of energy from the excited state of trimer ≡SiSiSi≡ clusters (6.7-eV absorption band) to the triplet T_1-state of ODC's also becomes possible.

Acknowledgments

The support of the Russian Education Agency (Program 'The development of scientific potential of higher school 2006–2008', Grant No. 2948), RFBR (Grant 08-02-00843) and HASYLAB (DESY) (Project II-04-068) are gratefully acknowledged.

References

[1] D.L. Griscom, in: G. Paccioni, L. Skuja, D.L. Griscom (Eds.), Defects in SiO_2 and Related Dielectrics: Science and Technology, NATO Science Series, Kluwer Academic, Dordrecht, 2000, p. 117.
[2] A.J. Cohen, Phys. Rev. 105 (1957) 1151.
[3] V. Garino-Canina, Comptes rendus Acad. Sci. 242 (1956) 1982.
[4] R. Tohmon, H. Mizuno, Y. Ohki, K. Sasagane, K. Nagasawa, Y. Hama, Phys. Rev. B 39 (1989) 1337.
[5] L. Skuja, Phys. Status Solidi (a) 114 (1989) 731.
[6] H. Hosono, Y. Abe, D. Kinser, R.A. Weeks, K. Muta, H. Kawazoe, Phys. Rev. B 46 (1992) 11445.
[7] J. Garapon, L. Favaro, B. Poumellec, J. Non-Cryst. Solids 353 (2007) 605.
[8] V.A. Radzig, J. Non-Cryst. Solids 239 (1998) 49.
[9] H.-J. Fitting, T. Barfels, A.N. Trukhin, B. Schmidt, A. Gulans, A. von Czarnowski, J. Non-Cryst. Solids 303 (2002) 218.
[10] A.F. Zatsepin, D.Yu. Biryukov, V.S. Kortov, S.Yu. Grohovskii, E.A. Buntov, Patent of the Russian Federation, Certificate No. 2006610036 (10 January 2006) of Official Computer Program Registration: Computer program for OSEE Spectroscopy Data Visualization ('Photoelectron').
[11] A.F. Zatsepin, D.Yu. Biryukov, V.S. Kortov, S.Yu. Grohovskii, E.A. Buntov, Patent of the Russian Federation, Certificate No. 2006610037 (10 January 2006) of Official Computer Program Registration: Computer Program for Processing and Analysis of OSEE Spectra ('Spectrograph').
[12] A.F. Zatsepin, D.Yu. Biryukov, V.S. Kortov, J. Appl. Spectrosc. 72 (2005) 407.
[13] A.F. Zatsepin, D.Yu. Biryukov, V.S. Kortov, Phys. Status Solidi (a) 202 (2005) 1935.
[14] I.A. Weinstein, A.F. Zatsepin, Phys. Status Solidi (c) 1 (2004) 2916.
[15] V.S. Kortov, A.F. Zatsepin, S.V. Gorbunov, A.M. Murzakaev, Phys. Solid State 48 (2006) 1273.
[16] L. Skuja, J. Non-Cryst. Solids 239 (1998) 16.
[17] A.F. Zatsepin, D.Yu. Biryukov, V.S. Kortov, Phys. Solid State 48 (2006) 245.
[18] A.F. Zatsepin, V.S. Kortov, H.-J. Fitting, J. Non-Cryst. Solids 351 (2005) 869.
[19] A.N. Trukhin, J. Jansons, H.-J. Fitting, T. Barfels, B. Schmidt, J. Non-Cryst. Solids 331 (2003) 91.
[20] Roushdey Salh, L. Fitting, E.V. Kolesnikova, A.A. Sitnikova, M.V. Zamoryanskaya, B. Schmidt, H.-J. Fitting, Semiconductors 41 (2007) 381.
[21] Roushdey Salh, L. Fitting Kourkoutis, B. Schmidt, H.-J. Fitting, Phys. Status Solidi (a) 204 (2007) 3132.
[22] A.F. Zatsepin, J. Non-Cryst. Solids 353 (2007) 590.
[23] H. Nishikawa, R. Tohmon, K. Nagasawa, Y. Hama, J. Appl. Phys. 65 (1989) 4672.
[24] R.A. Weeks, R.H. Magruder III, P. Wang, J. Non-Cryst. Solids 149 (1992) 122.
[25] V.A. Radtsig, Chem. Phys. 14 (1995) 125.